

Article

Tetrahydrofuran (THF)-Mediated Structure of $\text{THF}\cdot(\text{H}_2\text{O})_{n=1-10}$: A Computational Study on the Formation of the THF Hydrate

Jinxiang Liu ^{1,2,*} , Yujie Yan ³, Youguo Yan ⁴ and Jun Zhang ^{4,*}¹ School of Physics and Technology, University of Jinan, Jinan 250022, China² School of Petroleum Engineering, China University of Petroleum, Qingdao, Shandong 266580, China³ Shandong Academy of Environmental Science, Jinan 250013, China; yanyujiehappy@163.com⁴ School of Materials Science and Engineering, China University of Petroleum, Qingdao 266580, China; yyg@upc.edu.cn

* Correspondence: sps_liujx@ujn.edu.cn (J.L.); sps_zhang@hotmail.com (J.Z.)

Received: 28 December 2018; Accepted: 29 January 2019; Published: 31 January 2019



Abstract: Tetrahydrofuran (THF) is well known as a former and a promoter of clathrate hydrates, but the molecular mechanism for the formation of these compounds is not yet well understood. We performed ab initio calculations and ab initio molecular dynamics simulations to investigate the formation, structure, and stability of $\text{THF}\cdot(\text{H}_2\text{O})_{n=1-10}$ and its significance to the formation of the THF hydrate. Weak hydrogen bonds were found between THF and water molecules, and THF could promote water molecules from the planar pentagonal or hexagonal ring. As a promoter, THF could increase the binding ability of the CH_4 , CO_2 , or H_2 molecule onto a water face, but could also enhance the adsorption of other THF molecules, causing an enrichment effect.

Keywords: clathrate hydrate; tetrahydrofuran; formation; ab initio calculation

1. Introduction

Clathrate hydrates are ice-like crystalline compounds in which gas molecules are engaged in a host framework of water molecules, and they are widely found in permafrost and ocean floor sediments [1–3]. Up to now, three common types of methane hydrate structures have been identified [4,5]: The cubic structure I (sI), the cubic structure II (sII), and the hexagonal structure H (sH). The sI hydrate contains 2 small 5^{12} cages and 6 $5^{12}6^2$ cages per unit cell, and the sII hydrate has 16 5^{12} cages and 8 $5^{12}6^4$ cages in one unit cell. The unit cell of the sH hydrate has three 5^{12} cages, two $4^35^66^3$ cages, and one $5^{12}6^8$ cage. Over the past few decades, clathrate hydrates have been considerably studied for scientific interest and various potential industrial applications [6–9]. However, high pressure and low temperature are required in the formation of clathrate hydrates, which thus limits the development of hydrate-based technology [10–12].

Thankfully, tetrahydrofuran (THF) molecules can form the sII hydrate at about room temperature and pressure [13], which can serve as a proxy for developing hydrate technology. Because of their large molecular size, THF molecules only occupy the large $5^{12}6^4$ cages, leaving the small 5^{12} cages vacant. More importantly, THF has been recognized as one of the most popular promoter molecules [14–18], which greatly reduces the formation pressure and/or increases the formation temperature of the mixed hydrate containing THF and a second guest component. Florusse et al. [19] have reported that hydrogen clusters can be stabilized and stored at a reduced pressure within the clathrate hydrate lattice by adding THF, where the small cages are occupied by hydrogen clusters and the large cages are singly occupied by THF. Recently, experiments [20] have shown that THF can remarkably stabilize clathrate hydrates with multigas guests (CH_4 , C_2H_6 , and C_3H_8) in moderate conditions, and its

concentration can also affect the distribution and preferential occupation of specific guest species in the cages. However, the molecular mechanism of formation of these compounds is not yet well understood [21,22].

Based on computer simulation methods [23], several hypotheses have been proposed to illustrate the microprocess of hydrate nucleation and growth, including a labile cluster hypothesis [24,25], a local structuring hypothesis [26], a blob mechanism [27], and a cage adsorption hypothesis [28]. Further, Wu and coworkers [29] have carried out a molecular dynamics study of the growth of the THF-CH₄ binary hydrate, and found that the growth rate is dominated by the adsorption of CH₄ to the growing interface and the migration and rearrangement of THF at the interface. Alavi and coworkers [30] have studied the hydrogen bonding of THF in binary sII hydrates via molecular dynamics simulations, and suggested that the number and nature of the second guests can affect the probability of hydrogen bonding of THF. Liu et al. [31] have studied the formation of the 5¹²6⁴ cage in the THF hydrate by sampling thermodynamically stable structures on the potential surface. Nevertheless, there have been only a limited number of computer simulation studies that have examined the microscopic mechanism of the initial formation process of the THF hydrate, i.e., the formation of the cage precursors, and our knowledge is still far from being complete.

In this work, we studied the interactions between THF and water molecules in spontaneously forming binary clusters of THF·(H₂O)_{n=1–10} by performing ab initio calculations. The results showed that the hydrogen bonds between THF and water were relatively weak, with a maximum number of two water molecules hydrogen bonded with THF, but THF could facilitate the rearrangement of water molecules to form a pentagonal or hexagonal planar ring, which was responsible for the formation of a clathrate cage. Further, THF could significantly enhance the attraction of water faces to a second-guest component, which is helpful in understanding the promotion effects of THF on clathrate hydrates of various gas molecules.

2. Computational Details

To obtain the initial configurations, we first added 1 THF and 100 water molecules into a simulation box with a size of 14.60 × 14.60 × 14.60 Å³ and performed ab initio molecular dynamics simulations in the canonical ensemble. The equations of motion were integrated with a time step of 0.5 fs, and the system was coupled with a Nosé–Hoover chain thermostat [32] to a bath at 300 K. After an equilibration period of 3.0 ps, THF and its nearest neighboring water molecules, up to 10, were in turn extracted from the periodic boxes and were fully optimized in a vacuum at zero temperature. The frequency analysis confirmed that the optimized structures were minima on the potential energy surface. All simulations and geometry optimizations were carried out by the DMol³ program [33]. The Perdew–Burke–Ernzerhof (PBE) gradient-corrected exchange–correlation functional [34] and the triple numerical plus polarization (TNP) basis set [35] were applied. The effects of the functionals and the basis sets were considered, and the compared results are given in Figure S10, Table S2, and Table S3 (in the Supplementary Materials). The semi-empirical Tkatchenko–Scheffler scheme [36] was used to improve the description of noncovalent forces.

The stability of the system was evaluated by the stabilization energy per molecule (E_{sta}) involving the zero-point vibrational energy correction, which was defined by

$$E_{sta} = \frac{(E_{THF} + n \cdot E_{water}) - E_{total}}{n + 1}, \quad (1)$$

where E_{THF} , E_{water} , and E_{total} represent the energy of the THF molecule, the water molecule, and the whole system, respectively. The binding strength of the gas molecule to the cluster was characterized by the interaction energy (E_{int}), defined as

$$E_{int} = (E_{residue} + E_{gas}) - E_{total}, \quad (2)$$

where E_{gas} represents the energy of the CH_4 , CO_2 , or H_2 molecule, and $E_{residue}$ represents the energy of the whole system without the gas molecule.

3. Results and Discussion

3.1. THF-Mediated Formation of the Water Face

For a binary THF and water cluster ($n = 1-10$), five uncorrelated configurations were extracted from the equilibrated simulation trajectory (see Figure S1), and the optimized structures are given in Figure S2. The stabilization energies of all optimized $THF \cdot (H_2O)_{n=1-10}$ clusters are shown in Figure 1, and the lowest-energy structures are shown in Figure 2. To observe whether hydrogen bonds could form between THF and water molecules, we analyzed the distance between H atoms of THF and their nearest O atoms of water molecules (Table S1), but the hydrogen bond did not occur. Instead, a hydrogen bond formed between the O atom of THF and the H atoms of water molecules, with a bond length (O...H) of about ~ 1.694 Å. Obviously, THF could form two hydrogen bonds at most, with two water molecules above and/or below the plane of the THF ring.

For the lowest-energy structures of $THF \cdot (H_2O)_{n=1-10}$ clusters, the stabilization energy increased almost linearly with the number of water molecules. In detail, the formation of double hydrogen bonds involving two water molecules was energetically more favorable than the formation of a single hydrogen bond involving one water molecule, featuring a stabilization energy of 0.216 eV and 0.177 eV, respectively. For the $THF \cdot (H_2O)_3$ cluster, two water molecules formed two hydrogen bonds with THF, while the third water molecule formed one hydrogen bond with another water molecule. In the $THF \cdot (H_2O)_4$ cluster, three water molecules below the THF ring had a trend of forming a ternary ring, but such a process was inhibited because of the stereo-hindrance and hydrophobic effects of the THF ring. By sequential addition of one more water molecule, the water–water interactions were greatly enhanced, and a planar ternary ring of water molecules formed on one side of the THF ring for the $THF \cdot (H_2O)_5$ cluster. This suggested that a quasiplanar cyclic structure of the water molecules would be energetically favorable, agreeing well with the theoretical results of Shields et al. [37], and thus this structure would considerably occur during the formation of the clathrate cage. Further, the ternary face of water molecules was nearly parallel to the THF ring because of the hydrophobic interactions between THF and water. For the $THF \cdot (H_2O)_6$ cluster, there were two cyclic hydrogen bonded networks, that is, a pentagonal ring involving THF and four water molecules and a ternary ring involving three water molecules. Interestingly, the THF–water hydrogen bonds were nearly vertical to the plane composed of water molecules in the pentagonal ring, while three water molecules in the ternary ring were coplanar. The dihedral angle between two water faces was about 123.8° , which was in the range of the value of the neighbor faces in the clathrate hydrate ($119.9^\circ-133.3^\circ$), suggesting that the water molecules cooperatively organized into a stable structure.

In the case of $THF \cdot (H_2O)_7$, a single planar pentagonal ring of water face emerged and was roughly parallel to the THF ring, despite the formation of a THF–water hydrogen bond. This observation of THF–water cooperating toward ordering was similar to previous studies by Walsh et al. [22] that showed that methane molecules adsorbed on opposite sides of a pentagonal face of water molecules in the hydrate nucleation, which in turn allowed the adsorption of more water molecules. However, our observations showed that this initial structure formed through THF mediating the arrangement of water molecules instead of the formation of a pentagonal water face followed by adsorbing THF. For one more adsorbed water molecule, it preferentially inserted into the pentagonal water ring, leading to the formation of the hexagonal water face. The stabilization energy increased from 0.377 eV to 0.407 eV, implying that this process was energetically feasible.

By sequentially increasing the number of water molecules, we found that the cyclic rings composed of five or six water molecules were most likely to occur, while the larger cyclic rings were thermodynamically unstable. As a result, a cage-like structure gradually formed, just like $THF \cdot (H_2O)_{10}$. In contrast, we investigated the $CH_4 \cdot (H_2O)_{10}$, $CO_2 \cdot (H_2O)_{10}$, and $H_2 \cdot (H_2O)_{10}$ clusters by

the same procedure, and the optimized structures are shown in Figures S5, S7, and S9. The stabilization energy was 0.389 eV, 0.383 eV, and 0.350 eV for the most stable structures of $\text{CH}_4 \cdot (\text{H}_2\text{O})_{10}$, $\text{CO}_2 \cdot (\text{H}_2\text{O})_{10}$, and $\text{H}_2 \cdot (\text{H}_2\text{O})_{10}$ clusters, respectively. These values were much smaller than those of $\text{THF} \cdot (\text{H}_2\text{O})_{10}$ (0.448 eV), implying that THF was more thermodynamically feasible in rearranging water molecules to form a cage precursor. Further, we note that CH_4 , CO_2 , and H_2 were likely to promote the spontaneous formation of pentagonal water faces, but THF could induce the formation of both pentagonal and hexagonal faces, which explained how THF occupied the $5^{12}6^4$ cage in the sII hydrate.

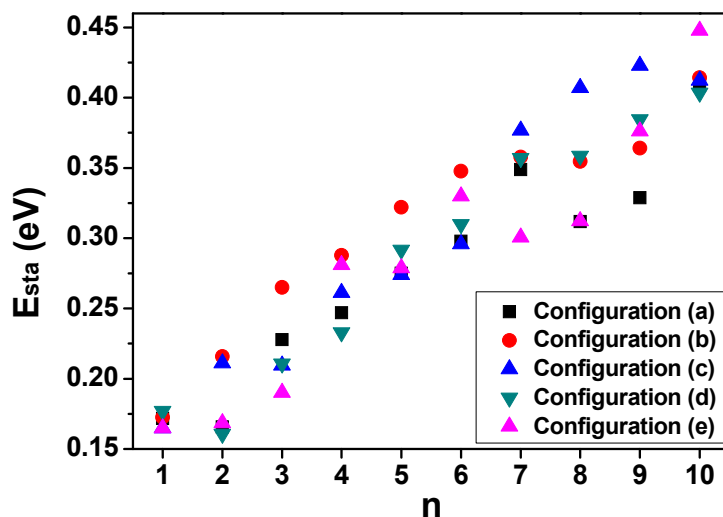


Figure 1. The stabilization energy (E_{sta} , with zero-point energy corrections) of binary $\text{THF} \cdot (\text{H}_2\text{O})_{n=1-10}$ clusters calculated at the Perdew–Burke–Ernzerhof (PBE) gradient-corrected exchange–correlation functional (PBE-D)/triple numerical plus polarization (TNP) level. The optimized geometries of $\text{THF} \cdot (\text{H}_2\text{O})_{n=1-10}$ clusters are given in Figure S2. THF: Tetrahydrofuran.

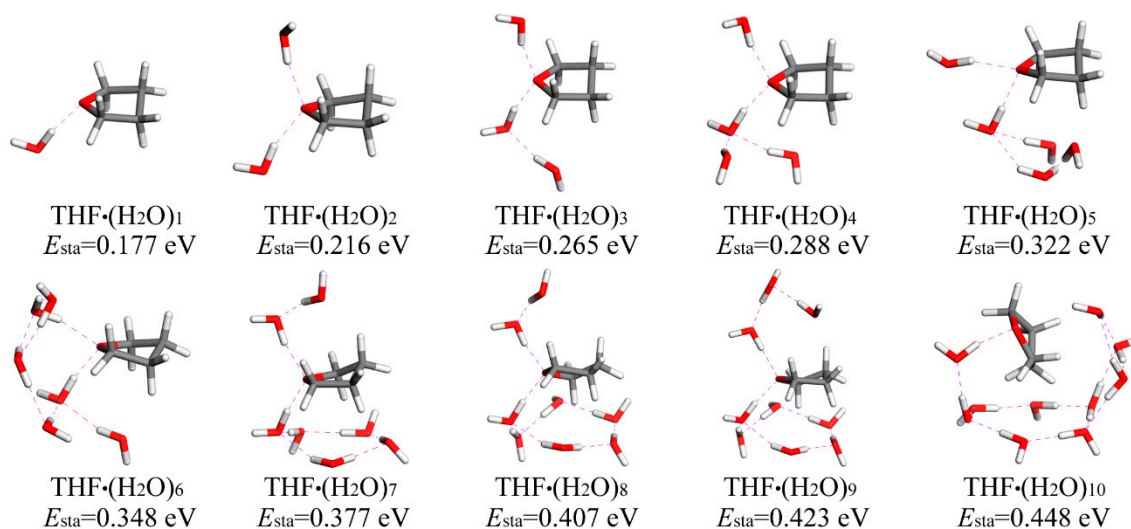


Figure 2. The most stable structures of binary $\text{THF} \cdot (\text{H}_2\text{O})_{n=1-10}$ clusters and their stabilization energies optimized at the PBE-D/TNP level. The hydrogen bonds are shown with violet dashed lines.

3.2. THF Enhanced the Binding Strength of a Gas Molecule

The above analysis suggests that THF could promote the formation and growth of water faces, and in the following part we will show that THF could also enhance the adsorption of a second gas molecule. First, we constructed a system consisting of THF and a pentagonal water ring and considered its attraction to CH_4 , CO_2 , H_2 , and other THF molecules. Figure 3 shows that there were two low-energy structures for $\text{THF} \cdot (\text{H}_2\text{O})_5$, where the THF ring was roughly vertical or parallel

to the pentagonal ring of water molecules, and the stabilization energy was 0.379 eV and 0.382 eV, respectively. This thus suggested that THF·(H₂O)₅ was likely to form a two-layer structure through a hydrogen bond between the O atom of THF and the H atom of a water molecule, in accordance with the aforementioned results.

The stabilization energy of the pentagonal water face plus a gas molecule (CH₄, CO₂, and H₂), the interaction energy, and the distance between them without and with adding an additional THF molecule are given in Table 1. The optimized structures of the pentagonal water face plus THF and a gas molecule are shown in Figure 3. It can be seen that CH₄ favored adsorbing on one side of the pentagonal water face and had a distance of 3.004 Å to the centroid of the pentagonal ring. The stabilization energy of this (CH₄)₁·(H₂O)₅ cluster was 0.325 eV, and the interaction energy between CH₄ and the pentagonal ring was 0.358 eV. Upon the addition of THF on the opposite side of the pentagonal water face, CH₄ became a little farther away from the pentagonal ring (3.100 Å), but the stability of the system was greatly enhanced ($E_{\text{sta}} = 0.346$ eV), and the attraction of the pentagonal ring to the CH₄ was also strengthened ($E_{\text{int}} = 0.362$ eV), thus improving the interactions between the pentagonal water faces and CH₄ molecules. Similarly, by adding THF, the distance between the pentagonal ring and CO₂ was elongated by 0.085 Å, and the stabilization energy was increased by 0.039 eV, which was almost equal to CH₄ (0.085 Å and 0.021 eV). However, the interaction energy between the pentagonal ring and CO₂ was considerably increased by 0.114 eV, implying that THF could more significantly improve the adsorption of CO₂ molecules than CH₄ molecules. In contrast, THF had little effect on the distance between the pentagonal ring and H₂ ($\Delta d = 0.017$ Å), because of the small size of H₂ molecules (non-heavy atom): However, the stabilization energy was increased by 0.061 eV, which was more significant than that of CH₄ and CO₂, although the interaction energy was just increased by 0.012 eV.

In the case of THF as a guest molecule, we found that two THF molecules favored adsorbing on opposite sides of the pentagonal water ring and retained their positions throughout the formation of hydrogen bonds with water molecules, leading to a sandwich structure, as shown in Figure 3. Interestingly, two THF molecules could not bind to one water molecule, agreeing well with the previous results of Shultz and Vu [38], which suggested that water did not form a bridging donor–donor structure with two THF molecules. Instead, the additional THF molecule joined with a different free water molecule, forming a cluster enriched in THF. From Table 1, we can see that the additional THF molecule enhanced the structural stability and the adsorption strength of the water face to THF, although THF had a larger distance to the water face. Therefore, THF was favorable for the pentagonal water face to adsorb CH₄, CO₂, H₂, or other THF molecules to form a cage precursor.

Subsequently, we constructed another system consisting of THF and a hexagonal water ring and considered its attraction to CH₄, CO₂, H₂, and other THF molecules. The stabilization energy of the hexagonal water face with a guest molecule (CH₄, CO₂, H₂, and THF), the interaction energy, and the distance between them without and with adding an additional THF molecule are given in Table 2. The optimized structures for all considered clusters are shown in Figure 4. It can be seen that the adsorbed THF ring could be either vertical or parallel to the hexagonal water face, with a stabilization energy of 0.384 eV and 0.392 eV, respectively. This indicated that THF was likely parallel to the hexagonal water face due to the formation of an extra hydrogen bond, which was similar to the case of the pentagonal water face. However, the THF became much closer to the hexagonal face than the pentagonal face (3.327 Å vs 3.431 Å), because the stereo-hindrance and hydrophilic–hydrophobic effects were weakened by the larger radius of the hexagonal ring.

For CH₄, CO₂, and H₂ molecules, they all preferentially located themselves along the central axis of the hexagonal water ring, and the distance between the center of the hexagonal ring and the guest molecule was 2.729, 2.715, and 2.161 Å, respectively. These distances were much smaller than the cases of the pentagonal water ring, which could be attributed to the weak stereo-hindrance effect caused by the large radius of the hexagonal ring. Upon adding one THF molecule on the opposite side of the hexagonal water ring, the distance was slightly elongated to 2.773, 2.749, and 2.276 Å for the CH₄,

CO₂, and H₂ molecules, respectively: The stabilization energy was increased by 0.024 eV, 0.019 eV, and 0.061 eV, respectively, and the interaction energy was increased by 0.006 eV, 0.082 eV, and 0.028 eV, respectively. These scenarios were quite similar to those of the pentagonal water ring, suggesting that THF could enhance the stability of the initial structure of the large cages but also improve the adsorption of CH₄, CO₂, and H₂ molecules to the hexagonal water face.

Table 1. The stabilization energy (E_{sta}), the interaction energy (E_{int}), and the distance (d) between the guest (CH₄, CO₂, H₂, and THF) and the pentagonal water ring calculated at the PBE-D/TNP level.

Guest	E_{sta} (eV)		E_{int} (eV)		d (Å)	
	without THF	with THF	without THF	with THF	without THF	with THF
CH ₄	0.325	0.346	0.358	0.362	3.004	3.100
CO ₂	0.326	0.365	0.389	0.502	2.861	2.946
H ₂	0.279	0.340	0.112	0.124	2.497	2.514
THF	0.382	0.399	0.812	0.816	3.431	3.481

Table 2. The stabilization energy (E_{sta}), the interaction energy (E_{int}), and the distance (d) between the guest (CH₄, CO₂, H₂, and THF) and the hexagonal water ring calculated at the PBE-D/TNP level.

Guest	E_{sta} (eV)		E_{int} (eV)		d (Å)	
	without THF	with THF	without THF	with THF	without THF	with THF
CH ₄	0.340	0.364	0.444	0.450	2.729	2.773
CO ₂	0.352	0.371	0.559	0.641	2.715	2.749
H ₂	0.294	0.355	0.128	0.156	2.161	2.276
THF	0.394	0.411	0.893	0.902	3.327	3.364

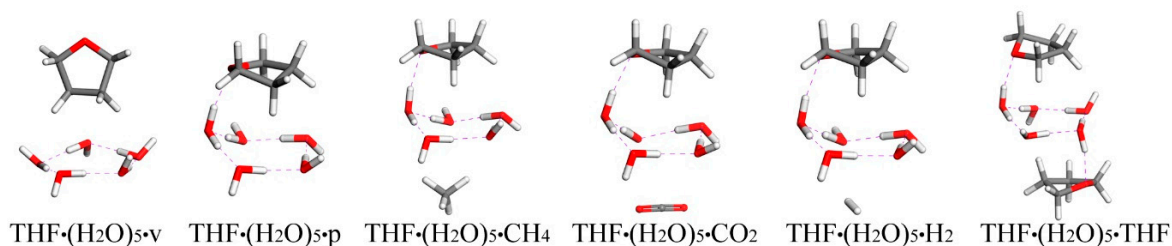


Figure 3. Low-energy structures of the clusters of THF plus a pentagonal ring of water molecules and/or CH₄/CO₂/H₂/THF optimized at the PBE-D/TNP level. The hydrogen bonds are shown with violet dashed lines.

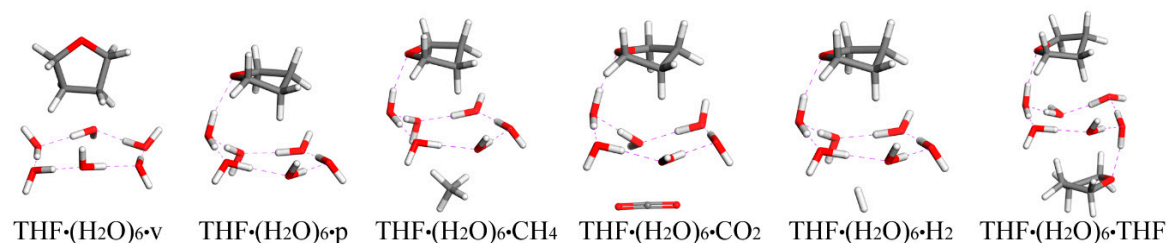


Figure 4. Low-energy structures of the clusters of THF plus a hexagonal ring of water molecules, and/or CH₄/CO₂/H₂/THF optimized at the PBE-D/TNP level. The hydrogen bonds are shown with violet dashed lines.

4. Conclusions

In the present work, we carried out ab initio studies of THF·(H₂O)_{n=1–10} clusters to reveal the initial process of the formation of the THF hydrate. Although THF had a weak hydrogen bond with water molecules, it could significantly promote the rearrangement of water molecules to form a planar

pentagonal or hexagonal ring, which was responsible for the formation of water faces of a clathrate cage. As a promoter, THF could greatly improve the stability of the cage precursors for the CH₄, CO₂, and H₂ hydrates and enhance the interactions between the water faces and these gas molecules. Further, our results also suggested that THF could facilitate the adsorption of other THF molecules, resulting in an enrichment effect.

Supplementary Materials: The following are available online at <http://www.mdpi.com/2073-4352/9/2/73/s1>, Figure S1. Initial configurations of five uncorrelated THF·(H₂O)_{n=1–10} clusters extracted from the ab initio molecular dynamics simulation trajectory. Figure S2. Optimized configurations of five uncorrelated THF·(H₂O)_{n=1–10} clusters. Figure S3. Labels of H atoms of the THF molecule. Figure S4. Initial configurations of five uncorrelated CH₄·(H₂O)₁₀ clusters, which were obtained by the same procedure as the THF·(H₂O)_{n=1–10} clusters. Figure S5. Optimized configurations of five uncorrelated CH₄·(H₂O)₁₀ clusters and their stabilization energies, optimized at the PBE-D/TNP level. Figure S6. Initial configurations of five uncorrelated CO₂·(H₂O)₁₀ clusters, which were obtained by the same procedure as the THF·(H₂O)_{n=1–10} clusters. Figure S7. Optimized configurations of five uncorrelated CO₂·(H₂O)₁₀ clusters and their stabilization energies, optimized at the PBE-D/TNP level. Figure S8. Initial configurations of five uncorrelated H₂·(H₂O)₁₀ clusters, which were obtained by the same procedure as the THF·(H₂O)_{n=1–10} clusters. Figure S9. Optimized configurations of five uncorrelated H₂·(H₂O)₁₀ clusters and their stabilization energies, optimized at the PBE-D/TNP level. Figure S10. The stabilization energies of the THF·(H₂O)_{n=1–10} clusters shown in Figure 2, calculated at the different levels. Table S1. The distance between H atoms of the THF molecule and their nearest O atoms of water molecules. Table S2. The stabilization energy (E_{sta}) of the pentagonal water ring plus a guest (CH₄, CO₂, H₂, and THF), calculated at the different functionals and basis sets. Table S3. The stabilization energy (E_{sta}) of the hexagonal water ring plus a guest (CH₄, CO₂, H₂, and THF), calculated at the different functionals and basis sets.

Author Contributions: Methodology, Y.Y. (Yujie Yan); investigation, Y.Y. (Youguo Yan) and J.Z.; writing—review and editing, J.L.

Funding: This work was supported by the National Natural Science Foundation of China [Grant number 11504133], the China Postdoctoral Science Foundation [Grant number 2017M612376], and the Postdoctoral Application Research Project of Qingdao [Grant number 2016216].

Conflicts of Interest: The authors declare no conflict of interest.

References

1. McMullan, R.K.; Jeffrey, G.A. Polyhedral Clathrate Hydrates. IX. Structure of Ethylene Oxide Hydrate. *J. Chem. Phys.* **1965**, *42*, 2725–2732. [[CrossRef](#)]
2. Mak, T.C.W.; McMullan, R.K. Polyhedral Clathrate Hydrates. X. Structure of the Double Hydrate of Tetrahydrofuran and Hydrogen Sulfide. *J. Chem. Phys.* **1965**, *42*, 2732–2737. [[CrossRef](#)]
3. Ripmeester, J.A.; Tse, J.S.; Ratcliffe, C.I.; Powell, B.M. A New Clathrate Hydrate Structure. *Nature* **1987**, *325*, 135–136. [[CrossRef](#)]
4. Sloan, E.D. Fundamental Principles and Applications of Natural Gas Hydrates. *Nature* **2003**, *426*, 353–363. [[CrossRef](#)] [[PubMed](#)]
5. Zhu, J.; Du, S.; Yu, X.; Zhang, J.; Xu, H.; Vogel, S.C.; Germann, T.C.; Francisco, J.S.; Izumi, F.; Momma, K.; et al. Encapsulation Kinetics and Dynamics of Carbon Monoxide in Clathrate Hydrate. *Nat. Commun.* **2014**, *5*, 4128. [[CrossRef](#)]
6. Dickens, G.R. A Methane Trigger for Rapid Warming? *Science* **2003**, *299*, 1017. [[CrossRef](#)]
7. Lee, H.; Lee, J.-W.; Kim, D.Y.; Park, J.; Seo, Y.-T.; Zeng, H.; Moudrakovski, I.L.; Ratcliffe, C.I.; Ripmeester, J.A. Tuning Clathrate Hydrates for Hydrogen Storage. *Nature* **2005**, *434*, 743–746. [[CrossRef](#)]
8. Liu, J.; Hou, J.; Xu, J.; Liu, H.; Chen, G.; Zhang, J. Ab Initio Study of the Molecular Hydrogen Occupancy in Pure H₂ and Binary H₂-THF Clathrate Hydrates. *Int. J. Hydrogen Energy* **2017**, *42*, 17136–17143. [[CrossRef](#)]
9. Sun, Q.; Kang, Y.T. Experimental Correlation for the Formation Rate of CO₂ Hydrate with THF (Tetrahydrofuran) for Cooling Application. *Energy* **2015**, *91*, 712–719. [[CrossRef](#)]
10. Yang, H.; Fan, S.; Lang, X.; Wang, Y. Phase Equilibria of Mixed Gas Hydrates of Oxygen+Tetrahydrofuran, Nitrogen+Tetrahydrofuran, and Air+Tetrahydrofuran. *J. Chem. Eng. Data* **2011**, *56*, 4152–4156. [[CrossRef](#)]
11. Mao, W.L.; Mao, H.-K.; Goncharov, A.F.; Struzhkin, V.V.; Guo, Q.; Hu, J.; Shu, J.; Hemley, R.J.; Somayazulu, M.; Zhao, Y. Hydrogen Clusters in Clathrate Hydrate. *Science* **2002**, *297*, 2247–2249. [[CrossRef](#)] [[PubMed](#)]
12. Shin, W.; Park, S.; Koh, D.-Y.; Seol, J.; Ro, H.; Lee, H. Water-Soluble Structure H Clathrate Hydrate Formers. *J. Phys. Chem. C* **2011**, *115*, 18885–18889. [[CrossRef](#)]

13. Makino, T.; Sugahara, T.; Ohgaki, K. Stability Boundaries of Tetrahydrofuran+Water System. *J. Chem. Eng. Data* **2005**, *50*, 2058–2060. [[CrossRef](#)]
14. Yang, M.; Jing, W.; Zhao, J.; Ling, Z.; Song, Y. Promotion of Hydrate-Based CO₂ Capture from Flue Gas by Additive Mixtures (THF (Tetrahydrofuran)+TBAB (Tetra-N-Butyl Ammonium Bromide)). *Energy* **2016**, *106*, 546–553. [[CrossRef](#)]
15. Koh, D.-Y.; Kang, H.; Lee, H. Multiple Guest Occupancy in Clathrate Hydrates and Its Significance in Hydrogen Storage. *Chem. Commun.* **2013**, *49*, 6782–6784.
16. Zhang, B.; Wu, Q. Thermodynamic Promotion of Tetrahydrofuran on Methane Separation from Low-Concentration Coal Mine Methane Based on Hydrate. *Energy Fuel* **2010**, *24*, 2530–2535. [[CrossRef](#)]
17. Alavi, S.; Ripmeester, J.A.; Klug, D.D. Molecular-Dynamics Simulations of Binary Structure II Hydrogen and Tetrahydrofurane Clathrates. *J. Chem. Phys.* **2006**, *124*, 014704. [[CrossRef](#)]
18. Lee, Y.-J.; Kawamura, T.; Yamamoto, Y.; Yoon, J.-H. Phase Equilibrium Studies of Tetrahydrofuran (THF)+CH₄, THF+CO₂, CH₄+CO₂, and THF+CO₂+CH₄ Hydrates. *J. Chem. Eng. Data* **2012**, *57*, 3543–3548. [[CrossRef](#)]
19. Florusse, L.J.; Peters, C.J.; Schoonman, J.; Hester, K.C.; Koh, C.A.; Dec, S.F.; Marsh, K.N.; Sloan, E.D. Stable Low-Pressure Hydrogen Clusters Stored in a Binary Clathrate Hydrate. *Science* **2004**, *306*, 469–471. [[CrossRef](#)]
20. Lee, S.; Lee, Y.; Park, S.; Kim, Y.; Cha, I.; Seo, Y. Stability Conditions and Guest Distribution of the Methane+Ethane+Propane Hydrates or Semiclathrates in the Presence of Tetrahydrofuran or Quaternary Ammonium Salts. *J. Chem. Thermodyn.* **2013**, *65*, 113–119.
21. Sosso, G.C.; Chen, J.; Cox, S.J.; Fitzner, M.; Pedevilla, P.; Zen, A.; Michaelides, A. Crystal Nucleation in Liquids: Open Questions and Future Challenges in Molecular Dynamics Simulations. *Chem. Rev.* **2016**, *116*, 7078–7116. [[CrossRef](#)] [[PubMed](#)]
22. Walsh, M.R.; Koh, C.A.; Sloan, E.D.; Sum, A.K.; Wu, D.T. Microsecond Simulations of Spontaneous Methane Hydrate Nucleation and Growth. *Science* **2009**, *326*, 1095–1098. [[CrossRef](#)] [[PubMed](#)]
23. English, N.J.; MacElroy, J.M.D. Perspectives on Molecular Simulation of Clathrate Hydrates: Progress, Prospects and Challenges. *Chem. Eng. Sci.* **2015**, *121*, 133–156. [[CrossRef](#)]
24. Sloan, E.D.; Fleyfel, F. A Molecular Mechanism for Gas Hydrate Nucleation from Ice. *AIChE J.* **1991**, *37*, 1281–1292. [[CrossRef](#)]
25. Christiansen, R.L.; Sloan, E.D. Mechanisms and Kinetics of Hydrate Formation. *Ann. N. Y. Acad. Sci.* **1994**, *715*, 283–305. [[CrossRef](#)]
26. Radhakrishnan, R.; Trout, B.L. A New Approach for Studying Nucleation Phenomena Using Molecular Simulations: Application to CO₂ Hydrate Clathrates. *J. Chem. Phys.* **2002**, *117*, 1786–1796. [[CrossRef](#)]
27. Jacobson, L.C.; Hujo, W.; Molinero, V. Amorphous Precursors in the Nucleation of Clathrate Hydrates. *J. Am. Chem. Soc.* **2010**, *132*, 11806–11811. [[CrossRef](#)]
28. Guo, G.-J.; Li, M.; Zhang, Y.-G.; Wu, C.-H. Why Can Water Cages Adsorb Aqueous Methane? A Potential of Mean Force Calculation on Hydrate Nucleation Mechanisms. *Phys. Chem. Chem. Phys.* **2009**, *11*, 10427–10437. [[CrossRef](#)]
29. Wu, J.-Y.; Chen, L.-J.; Chen, Y.-P.; Lin, S.-T. Molecular Dynamics Study on the Growth Mechanism of Methane Plus Tetrahydrofuran Mixed Hydrates. *J. Phys. Chem. C* **2015**, *119*, 19883–19890. [[CrossRef](#)]
30. Alavi, S.; Ripmeester, J.A. Effect of Small Cage Guests on Hydrogen Bonding of Tetrahydrofuran in Binary Structure II Clathrate Hydrates. *J. Chem. Phys.* **2012**, *137*, 054712. [[CrossRef](#)]
31. Liu, J.; Shi, S.; Zhang, Z.; Liu, H.; Xu, J.; Chen, G.; Hou, J.; Zhang, J. Ab Initio Study of Formation of the Clathrate Cage in the Tetrahydrofuran Hydrate. *J. Chem. Thermodyn.* **2018**, *120*, 39–44. [[CrossRef](#)]
32. Nosé, S. A Molecular Dynamics Method for Simulations in the Canonical Ensemble. *Mol. Phys.* **1984**, *52*, 255–268. [[CrossRef](#)]
33. Tang, L.-G.; Li, X.-S.; Feng, Z.-P.; Li, G.; Fan, S.-S. Control Mechanisms for Gas Hydrate Production by Depressurization in Different Scale Hydrate Reservoirs. *Energy Fuel* **2007**, *21*, 227–233. [[CrossRef](#)]
34. Perdew, J.P.; Burke, K.; Ernzerhof, M. Generalized Gradient Approximation Made Simple. *Phys. Rev. Lett.* **1996**, *77*, 3865–3868. [[CrossRef](#)] [[PubMed](#)]
35. Delley, B. Ground-State Enthalpies: Evaluation of Electronic Structure Approaches with Emphasis on the Density Functional Method. *J. Phys. Chem. A* **2006**, *110*, 13632–13639. [[CrossRef](#)] [[PubMed](#)]
36. Tkatchenko, A.; Scheffler, M. Accurate Molecular Van Der Waals Interactions from Ground-State Electron Density and Free-Atom Reference Data. *Phys. Rev. Lett.* **2009**, *102*, 073005. [[CrossRef](#)] [[PubMed](#)]

37. Cox, S.J.; Towler, M.D.; Alfè, D.; Michaelides, A. Benchmarking the Performance of Density Functional Theory and Point Charge Force Fields in Their Description of Si Methane Hydrate against Diffusion Monte Carlo. *J. Chem. Phys.* **2014**, *140*, 174703. [[CrossRef](#)]
38. Shultz, M.J.; Vu, T.H. Hydrogen Bonding between Water and Tetrahydrofuran Relevant to Clathrate Formation. *J. Phys. Chem. B* **2015**, *119*, 9167–9172. [[CrossRef](#)]



© 2019 by the authors. Licensee MDPI, Basel, Switzerland. This article is an open access article distributed under the terms and conditions of the Creative Commons Attribution (CC BY) license (<http://creativecommons.org/licenses/by/4.0/>).